Resonant laser printing of bi-material metasurfaces: from plasmonic to photonic optical response

Raza, Søren; Lavieja, Cristian; Zhu, Xiaolong; Kristensen, Anders

Published in:
Optics Express

Link to article, DOI:
10.1364/OE.26.020203

Publication date:
2018

Document Version
Publisher's PDF, also known as Version of record

Research Article | Vol. 26, No. 16 | 6 Aug 2018 | OPTICS EXPRESS 20203
Optics EXPRESS

Resonant laser printing of bi-material metasurfaces: from plasmonic to photonic optical response

SØREN RAZA,[1,3] CRISTIAN LAVIEJA,[1,2,3] XIAOLONG ZHU,[1] AND ANDERS KRISTENSEN[1,*]

[1]*Department of Micro and Nanotechnology, Technical University of Denmark, DK-2800 Kongens Lyngby, Denmark*
[2]*Instituto de Ciencia de Materiales de Aragón (ICMA), University of Zaragoza, 50018 Zaragoza, Spain*
[3]*These authors contributed equally to this work*
[*]*anders.kristensen@nanotech.dtu.dk*

Abstract: Metasurfaces are nanostructured surfaces with engineered optical properties - currently impacting many branches of optics, from miniaturization of optical components to realizing high-resolution structural colors. The optical properties of metasurfaces can be traced to the individual meta-atoms, which set the nature of the optical response, e.g., plasmonic for metallic meta-atoms or photonic for dielectric meta-atoms. Combining multiple types of responses opens up new horizons in design of optical materials, but has so far been avoided due to the fabrication difficulties associated with constructing a metasurface composed of several meta-atom materials. Here, we present a multi-material design approach by optically post-processing a metasurface constructed from self-assembled polystyrene spheres coated with silver. Using our concept of resonant laser printing, we locally alter the initial plasmonic response of the meta-atoms to a pure photonic response. Our work constitutes a conceptually different way of designing metasurfaces and can pave the way for realizing multi-material metasurfaces on large areas while being cost effective.

OCIS codes: (160.3918) Metamaterials; (250.5403) Plasmonics; (350.4238) Nanophotonics and photonic crystals; (140.3390) Laser materials processing.

References and links

1. A. Pors, M. G. Nielsen, R. L. Eriksen, and S. I. Bozhevolnyi, "Broadband focusing flat mirrors based on plasmonic gradient metasurfaces," Nano Lett. **13**, 829–834 (2013).
2. A. V. Kildishev, A. Boltasseva, and V. M. Shalaev, "Planar photonics with metasurfaces," Science. **339**, 1232009 (2013).
3. N. Yu and F. Capasso, "Flat optics with designer metasurfaces," Nat. Mater. **13**, 139–150 (2014).
4. D. Lin, P. Fan, E. Hasman, and M. L. Brongersma, "Dielectric gradient metasurface optical elements," Science. **345**, 298–302 (2014).
5. S. Jahani and Z. Jacob, "All-dielectric metamaterials," Nat. Nanotechnol. **11**, 23–36 (2016).
6. I. Staude and J. Schilling, "Metamaterial-inspired silicon nanophotonics," Nat. Photonics **11**, 274–284 (2017).
7. K. Kumar, H. Duan, R. S. Hegde, S. C. W. Koh, J. N. Wei, and J. K. W. Yang, "Printing colour at the optical diffraction limit," Nat. Nanotechnol. **7**, 557–561 (2012).
8. X. Ni, Z. J. Wong, M. Mrejen, Y. Wang, and X. Zhang, "An ultrathin invisibility skin cloak for visible light," Science. **349**, 1310–1314 (2015).
9. M. Khorasaninejad, W. T. Chen, R. C. Devlin, J. Oh, A. Y. Zhu, and F. Capasso, "Metalenses at visible wavelengths: Diffraction-limited focusing and subwavelength resolution imaging," Science. **352**, 1190–1194 (2016).
10. W. T. Chen, A. Y. Zhu, V. Sanjeev, M. Khorasaninejad, Z. Shi, E. Lee, and F. Capasso, "A broadband achromatic metalens for focusing and imaging in the visible," Nat. Nanotechnol. **13**, 220–226 (2018).
11. O. Avayu, E. Almeida, Y. Prior, and T. Ellenbogen, "Composite functional metasurfaces for multispectral achromatic optics," Nat. Commun. **8**, 14992 (2017).
12. F. Ding, A. Pors, and S. I. Bozhevolnyi, "Gradient metasurfaces: a review of fundamentals and applications," Rep. Prog. Phys. **81**, 026401 (2018).
13. X. Zhu, C. Vannahme, E. Højlund-Nielsen, N. A. Mortensen, and A. Kristensen, "Plasmonic colour laser printing," Nat. Nanotechnol. **11**, 325–329 (2016).

#332411 https://doi.org/10.1364/OE.26.020203
Journal © 2018 Received 23 May 2018; revised 22 Jun 2018; accepted 22 Jun 2018; published 25 Jul 2018

Optics EXPRESS

14. X. Zhu, W. Yan, U. Levy, N. A. Mortensen, and A. Kristensen, "Resonant laser printing of structural colors on high-index dielectric metasurfaces," Sci. Adv. **3**, e1602487 (2017).
15. X. Zhu, M. K. Hedayati, S. Raza, U. Levy, N. A. Mortensen, and A. Kristensen, "Digital resonant laser printing: Bridging nanophotonic science and consumer products," Nano Today **19**, 7–10 (2018).
16. X. Zhu, L. Shi, X. Liu, J. Zi, and Z. Wang, "A mechanically tunable plasmonic structure composed of a monolayer array of metal-capped colloidal spheres on an elastomeric substrate," Nano Res. **3**, 807–812 (2010).
17. L. Shi, H. Yin, X. Zhu, X. Liu, and J. Zi, "Direct observation of iso-frequency contour of surface modes in defective photonic crystals in real space," Appl. Phys. Lett. **97**, 251111 (2010).
18. J. Sun, C.-j. Tang, P. Zhan, Z.-l. Han, Z.-S. Cao, and Z.-L. Wang, "Fabrication of centimeter-sized single-domain two-dimensional colloidal crystals in a wedge-shaped cell under capillary forces," Langmuir. **26**, 7859–7864 (2010).
19. M. S. Carstensen, X. Zhu, O. E. Iyore, N. A. Mortensen, U. Levy, and A. Kristensen, "Holographic resonant laser printing of flat optics using template plasmonic metasurfaces," ACS Photonics **5**, 1665–1670 (2017).
20. X. Chen, Y. Chen, M. Yan, and M. Qiu, "Nanosecond photothermal effects in plasmonic nanostructures," ACS Nano **6**, 2550–2557 (2012).
21. G. Baffou and R. Quidant, "Thermo-plasmonics: using metallic nanostructures as nano-sources of heat," Laser Photonics Rev. **7**, 171–187 (2013).
22. D. E. Aspnes and A. A. Studna, "Dielectric functions and optical parameters of Si, Ge, GaP, GaAs, GaSb, InP, InAs, and InSb from 1.5 to 6.0 eV," Phys. Rev. B **27**, 985–1009 (1983).
23. P. B. Johnson and R.-W. Christy, "Optical constants of the noble metals," Phys. Rev. B **6**, 4370–4379 (1972).
24. C. Farcau, M. Giloan, E. Vinteler, and S. Astilean, "Understanding plasmon resonances of metal-coated colloidal crystal monolayers," Appl. Phys. B **106**, 849–856 (2012).
25. J. S. Clausen, E. Højlund-Nielsen, A. B. Christiansen, S. Yazdi, M. Grajower, H. Taha, U. Levy, A. Kristensen, and N. A. Mortensen, "Plasmonic metasurfaces for coloration of plastic consumer products," Nano Lett. **14**, 4499–4504 (2014).
26. S. J. Tan, L. Zhang, D. Zhu, X. M. Goh, Y. M. Wang, K. Kumar, C.-W. Qiu, and J. K. W. Yang, "Plasmonic color palettes for photorealistic printing with aluminum nanostructures," Nano Lett. **14**, 4023–4029 (2014).
27. A. S. Roberts, A. Pors, O. Albrektsen, and S. I. Bozhevolnyi, "Subwavelength plasmonic color printing protected for ambient use," Nano Lett. **14**, 783–787 (2014).
28. J. Olson, A. Manjavacas, L. Liu, W.-S. Chang, B. Foerster, N. S. King, M. W. Knight, P. Nordlander, N. J. Halas, and S. Link, "Vivid, full-color aluminum plasmonic pixels," Proc. Natl. Acad. Sci. **111**, 14348–14353 (2014).
29. E. Højlund-Nielsen, X. Zhu, M. S. Carstensen, M. K. Sørensen, C. Vannahme, N. A. Mortensen, and A. Kristensen, "Polarization-dependent aluminum metasurface operating at 450 nm," Opt. Express **23**, 28829–28835 (2015).
30. F. Cheng, J. Gao, T. S. Luk, and X. Yang, "Structural color printing based on plasmonic metasurfaces of perfect light absorption," Sci. Rep. **5**, 11045 (2015).
31. Y. Shen, V. Rinnerbauer, I. Wang, V. Stelmakh, J. D. Joannopoulos, and M. Soljačić, "Structural colors from Fano resonances," ACS Photonics **2**, 27–32 (2015).
32. J. Proust, F. Bedu, B. Gallas, I. Ozerov, and N. Bonod, "All-dielectric colored metasurfaces with silicon Mie resonators," ACS Nano **10**, 7761–7767 (2016).
33. Z. Li, W. Wang, D. Rosenmann, D. A. Czaplewski, X. Yang, and J. Gao, "All-metal structural color printing based on aluminum plasmonic metasurfaces," Opt. Express **24**, 20472–20480 (2016).
34. X. M. Goh, R. J. H. Ng, S. Wang, S. J. Tan, and J. K. Yang, "Comparative study of plasmonic colors from all-metal structures of posts and pits," ACS Photonics **3**, 1000–1009 (2016).
35. L. Wang, R. J. H. Ng, S. Safari Dinachali, M. Jalali, Y. Yu, and J. K. W. Yang, "Large area plasmonic color palettes with expanded gamut using colloidal self-assembly," ACS Photonics **3**, 627–633 (2016).
36. R. Yu, P. Mazumder, N. F. Borrelli, A. Carrilero, D. S. Ghosh, R. A. Maniyara, D. Baker, F. J. García de Abajo, and V. Pruneri, "Structural coloring of glass using dewetted nanoparticles and ultrathin films of metals," ACS Photonics **3**, 1194–1201 (2016).
37. S. Sun, Z. Zhou, C. Zhang, Y. Gao, Z. Duan, S. Xiao, and Q. Song, "All-dielectric full-color printing with TiO2 metasurfaces," ACS Nano **11**, 4445–4452 (2017).
38. A. Kristensen, J. K. Yang, S. I. Bozhevolnyi, S. Link, P. Nordlander, N. J. Halas, and N. A. Mortensen, "Plasmonic colour generation," Nat. Rev. Mater. **2**, 16088 (2016).
39. V. R. Shrestha, S.-S. Lee, E.-S. Kim, and D.-Y. Choi, "Polarization-tuned dynamic color filters incorporating a dielectric-loaded aluminum nanowire array," Sci. Rep. **5**, 12450 (2015).
40. L. Duempelmann, A. Luu-Dinh, B. Gallinet, and L. Novotny, "Four-fold color filter based on plasmonic phase retarder," ACS Photonics **3**, 190–196 (2016).
41. S. Yokogawa, S. P. Burgos, and H. A. Atwater, "Plasmonic color filters for CMOS image sensor applications," Nano Lett. **12**, 4349–4354 (2012).
42. S. Murthy, H. Pranov, N. A. Feidenhans, J. S. Madsen, P. E. Hansen, H. C. Pedersen, and R. Taboryski, "Plasmonic color metasurfaces fabricated by a high speed roll-to-roll method," Nanoscale. **9**, 14280–14287 (2017).
43. A. I. Kuznetsov, A. E. Miroshnichenko, M. L. Brongersma, Y. S. Kivshar, and B. Luk' yanchuk, "Optically resonant dielectric nanostructures," Science. **354**, 6314 (2016).
44. A. L. Holsteen, S. Raza, P. Fan, P. G. Kik, and M. L. Brongersma, "Purcell effect for active tuning of light scattering from semiconductor optical antennas," Science. **358**, 1407–1410 (2017).

Optics EXPRESS

1. Introduction

Optical metasurfaces are currently receiving tremendous attention from the nanophotonics community due to their prospects in creating new optical functionalities and miniaturizing existing optoelectronic devices [1–6]. Many exciting applications have already been realized, such as carpet cloaking, high-numerical-aperture lenses, and structural colors [7–10]. The metasurfaces are typically fabricated by top-down nanolithography, where meta-atoms of specific shape, size, and material, are placed periodically on a substrate. The top-down approach is costly and intricate as it involves electron-beam lithography to ensure subwavelength meta-atom sizes, and as such often excludes metasurfaces consisting of meta-atoms of several materials. However, multi-material metasurfaces are promising for broadband performance [11] and for realizing different functionalities at different wavelengths. As an example, multi-material metasurfaces open up the possibility of combining Huygen's metasurfaces with plasmonic metasurfaces [12] to realize, e.g., highly directional phase-gradient metasurfaces. In general, multi-material metasurfaces offer an interesting design knob by being able to combine localized plasmon and high-refractive-index Mie resonances with delocalized photonic-crystal resonances.

Realizing different types of optical responses within a single metasurface is unprecedented, largely because of the fabrication difficulties associated with it. Here, we introduce a conceptually simple approach to designing multi-material metasurfaces. Instead of pre-designing an inhomogeneous metasurface with meta-atoms of different materials at different positions (top-down approach), we prepare a homogeneous metasurface where each meta-atom is identical and consists of two materials. By using resonant laser printing [13–15] we optically post-process our bi-material metasurfaces to change the ratio of the two materials. Our approach allows us to avoid top-down lithography altogether and we therefore prepare our metasurface using self-assembled polystyrene spheres (bottom-up approach) [16, 17], which are subsequently coated with silver. The optical response of the silver-coated polystyrene spheres is dominated by a localized plasmon resonance. Depending on the pulse energy, resonant laser printing locally deforms or ablates the silver coating, which reveals the delocalized photonic-crystal response of the polystyrene spheres. The result is a bi-material metasurface consisting of meta-atoms of varying amount of silver-to-polystyrene material, which we use to create structural colors with high resolution (over 20.000 dots per inch).

2. Results and discussion

The laser processing of our self-assembled metasurface is schematically shown in Fig. 1(a). The metasurface is prepared by confining the polystyrene nanoparticle suspension (400 nm, diameter) with capillary forces using two parallel glass slides. We use a rectangular wedge-shaped cell with three open sides, which ensures that the contact drying front of the colloidal suspension forms a convex curve. As the solvent evaporates the convective flow lines up the polystyrene spheres to the drying front to create a hexagonal lattice [18]. Subsequently, we sputter 30 nm of silver on the polystyrene hexagonal lattice, which results in a dome-shaped silver layer on top of the polystyrene particles, see Fig. 1(a). The silver layer induces a purely plasmonic response of the metasurface, which can be seen from the localization of the electric field to the silver capping layer [Fig. 1(b)]. Post-processing the metasurface with a pulsed laser allows us to gradually change the optical response from plasmonic to more photonic by reshaping the silver cap. With sufficiently large pulse energies, we can ablate the silver cap, which leads to a purely photonic response where the reflection dip occurs due to a weak Fabry–Pérot-type resonance in the polystyrene spheres [Fig. 1(c)].

We design the metasurface using a laser-processing technique known as digital resonant laser printing (DRLP) [13–15, 19]. Here, the silver layer is reshaped by briefly heating it above its melting temperature using a nanosecond-pulsed laser [20, 21], see Fig. 2. By using a laser with a

Optics EXPRESS

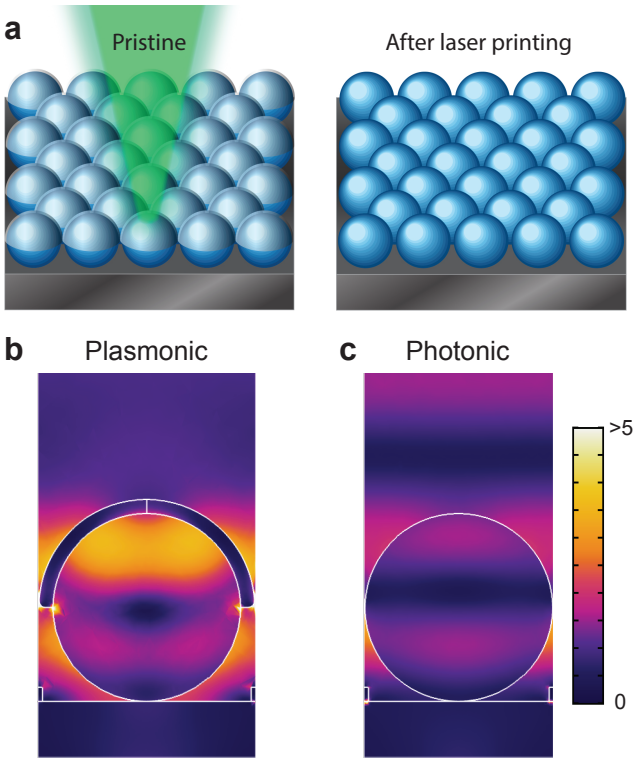

Fig. 1. (a) Schematic of the laser processing of our self-assembled metasurface. (b-c) Simulated electric field norms of the two main reflection dips of the pristine and completely post-processed areas, respectively.

wavelength close to the localized surface plasmon (LSP) resonance, we can spatially localize the heating process due to the strong electric field confinement of the LSPs. The spatial resolution of DRLP is a convolution of the Gaussian distribution of the laser beam and the nanoscale electric field confinement of LSPs, which can lead to sub-diffraction resolution [14]. For our bi-material metasurface, the electric field is strongly localized in the gap between neighboring polystyrene spheres [Fig. 1(b)], limiting our DRLP resolution to approximately 800 nm (corresponding to the diameter of two spheres).

With DRLP, we can controllably transition the metasurface from the plasmonic response of the silver cap to a photonic-crystal response of the polystyrene spheres. DRLP melts the edges of the silver cap, which reduces their size, while leaving the polystyrene spheres unchanged [Fig. 2(a)-(e)]. The degree of the reshaping is tuned by the laser pulse energy. We use pulse energies between 0 and 30 nJ, since energies above lead to ablation of the polystyrene spheres. With a pulse energy of 30 nJ the silver is ablated [Fig. 2(e)], leading to the photonic state where the optical response is only due to the polystyrene spheres. The reshaping of the silver layer induces a clear change in the visible reflected color [Fig. 2(f)-(j)]. When viewed through a 20× microscope objective the color changes from an initial blue to purple and then finally to white. The reflectance spectra, which are collected over a large area of $500 \times 500\ \mu m^2$ to average out the local inhomogeneity, also show a significant change with pulse energy [Fig. 2(k)-(o)]. In the pristine case, the main reflection dip, which is due to the LSP, occurs just below 600 nm [Fig. 2(k)]. For low pulse energies, the silver cap becomes smaller, which leads to a slight blueshift in the LSP resonance and an overall lower reflectance [Fig. 2(l)-(m)]. As the pulse energy increases,

Optics EXPRESS

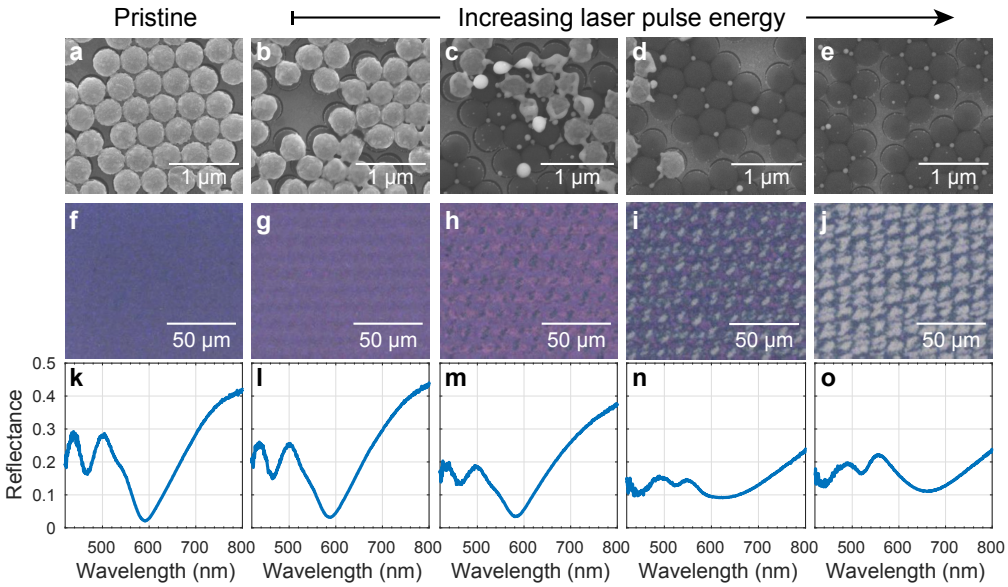

Fig. 2. (a-e) SEM and (f-j) optical bright-field images with (k-o) corresponding reflectance measurements of post-processed areas of the self-assembled metasurface. The regions have been reshaped using a 1-ns-pulsed green laser (532 nm wavelength) with pulse energies increasing from 0 nJ to 30 nJ.

the amount of silver decreases, which reveals the optical response of the polystyrene spheres [Fig. 2(n)-(o)]. Here, a redshift of the main reflection is observed accompanied by an additional reduction in overall reflectance.

To gain a detailed understanding of the experimentally observed reflectance dips, we perform three-dimensional full-field simulations (COMSOL v. 5.2a) of the pristine and completely-processed (i.e., ablated silver) states of our metasurface, see Fig. 3. Simulations of the intermediate states (i.e., pulse energies less than 30 nJ) are complicated by the lack of periodicity [see Fig. 2(b)-(e)]. We therefore focus on the pristine (0 nJ) and completely-processed states (30 nJ), where we account for the hexagonal symmetry. We excite the metasurface with a normally-incident plane wave polarized along the y direction and propagating in the negative z direction. The polystyrene sphere, which is placed on an optically-thick silicon substrate, has a diameter of 400 nm and is coated with a 30 nm thick silver hemi-spherical cap. For polystyrene we use a constant refractive index of 1.59, while for silver and silicon we use the wavelength-dependent refractive indices reported in literature [22, 23].

In the pristine case [Fig. 3(a)], we find three reflectance dips, in accordance with experiments. The main dip occurs at a wavelength of 585 nm and is due to the excitation of a LSP, as can be seen from the electric field profile shown as an inset. The shorter wavelength reflectance dips at 535 nm and 470 nm are due to excitation of surface waves in the plane of the periodic hexagonal metasurface, [24] where the former is still weakly influenced by the LSP (see electric field insets). Despite an overall larger reflectance in the simulations, we find that the wavelengths of the reflectance dips are in excellent agreement with the experiments. In the completely-processed state, where the silver cap is removed, the structure is essentially a photonic crystal [Fig. 3(b)]. Here, the main reflectance dip occurs at a longer wavelength of 670 nm. From the electric field profile and power flow arrows, we can see that the dip occurs due to a weak Fabry–Pérot-type resonance in the polystyrene spheres. At a shorter wavelength of 495 nm, another reflectance dip is observed, which is due to the excitation of a (delocalized) surface wave in the plane

Optics EXPRESS

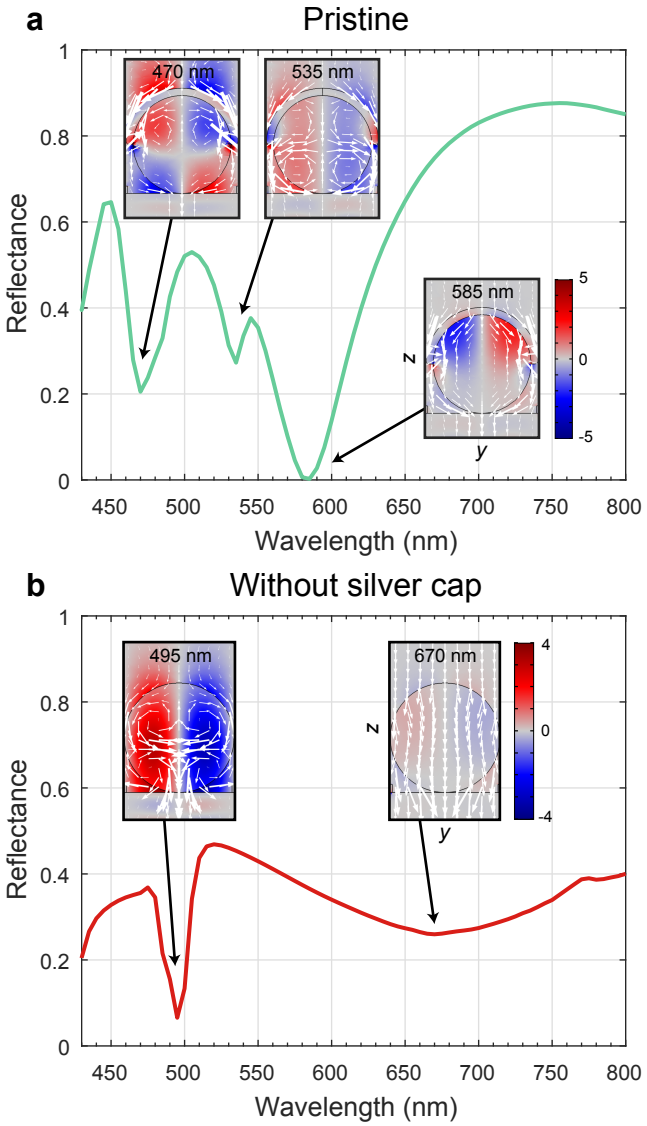

Fig. 3. (a) Full-field 3D simulation of the reflectance spectrum of the pristine self-assembled metasurface, accounting for both the optically-thick silicon substrate and the hexagonal symmetry of the metasurface. The insets show the z-component (normal to the substrate) of the electric field at the wavelengths of the reflection dips. The Poynting vectors are superimposed as white arrows to illustrate the electromagnetic power flow. (b) Similar to (a) but for the case where the entire hemi-spherical silver cap has been removed by resonant laser printing.

of the photonic crystal. From the electric field profile, we see that this mode resembles the surface wave seen for the pristine case at 535 nm. The resonance wavelength is shorter in the completely-processed case, because the periodicity is decreased due to the removal of the silver cap. The simulated reflectance spectrum is in good agreement with the experiments, although we observe an additional dip at shorter wavelengths in the experiments which is not captured in the simulations. We interpret this as a higher-order surface wave related to the periodic hexagonal

Optics EXPRESS

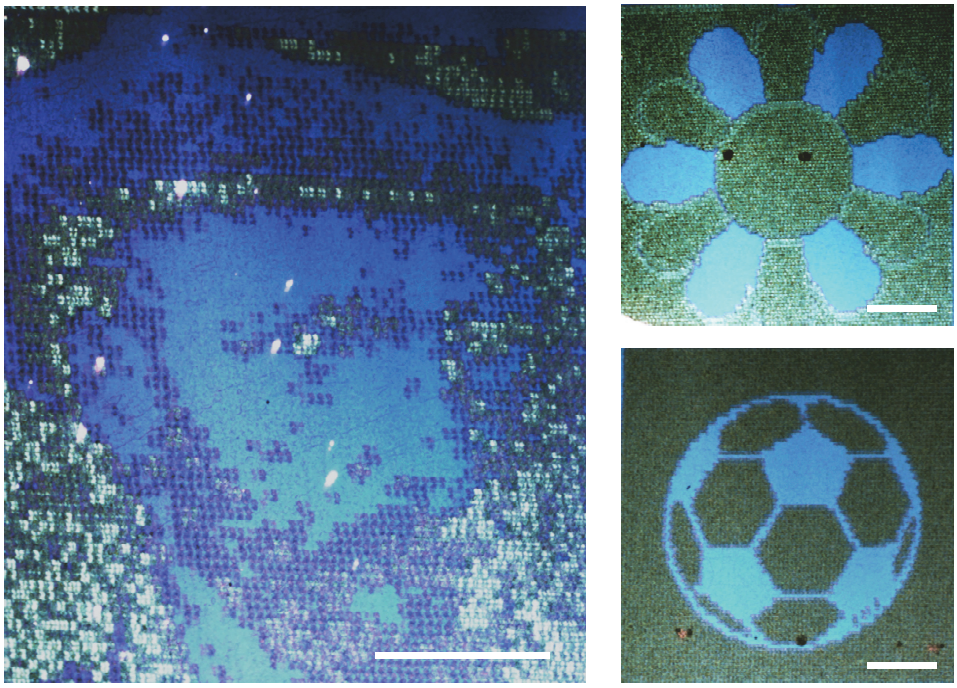

Fig. 4. Examples of structural colors created by gradually changing the optical response of the bi-material metasurface from plasmonic to photonic using resonant laser printing. Scale bars: 1 mm.

structure of the metasurface. Overall, the simulations accurately capture the features observed in the experiments and reveal that the initial plasmonic response of the pristine state is transformed to a photonic-crystal response by DRLP.

We use our bi-material metasurface design approach to realize high-resolution structural colors (Fig. 4). Structural colors based on metal or semi-conductor metasurfaces [25–37] have huge potential for use in surface decorations [7, 38] and color filters [39–41] and have already been upscaled using roll-to-roll methods [42]. Our bi-material metasurface can be manipulated using DRLP to draw any desired image (Fig. 4). The image printing is fully automatic, where our software controls and synchronizes the movements of a mechanical stage and a beam polarizer where the latter controls the laser pulse energy. The different colors are achieved by varying the pulse energy at different locations, as explained in relation to Fig. 2. This results in local modifications of the silver-to-polystyrene ratio, which locally changes the optical response from plasmonic to photonic, enabling us to realize high-resolution color printing.

3. Conclusions

We have introduced a conceptually simple design approach to realizing multi-material metasurfaces. The metasurface is initially prepared by homogeneously patterning the surface with two materials (polystyrene and silver) and then post-processed using nanosecond laser pulses to define meta-atoms of varying polystyrene-to-silver ratio. We show that this powerful approach allows us to avoid top-down lithography and can be used to realize large-area structural colors with high resolution. The approach can be easily extended to more than two materials, including combinations of metals and high-refractive-index materials [43, 44], thereby extending the palette

Optics EXPRESS

of metasurface possibilities.

Funding

Independent Research Funding Denmark (7026-00117B); VILLUM FONDEN (17400).

Acknowledgments

The authors would like to thank Prof. Jian Zi from Fudan University for fruitful discussions. S. R. acknowledges support by the Independent Research Funding Denmark (7026-00117B). X. Z. acknowledges the supporting of VILLUM Experiment (Grant No. 17400) from VILLUM FONDEN.

Disclosures

The authors declare that there are no conflicts of interest related to this article.